

# Probing small $x(g)$ region with the LHeC based $\gamma p$ colliders

U. Kaya<sup>1</sup>, S. Sultansoy<sup>1,2</sup>, G. Unel<sup>3</sup>

<sup>1</sup>*TOBB University of Economics and Technology, Ankara, Turkey*

<sup>2</sup>*ANAS Institute of Physics, Baku, Azerbaijan*

<sup>3</sup>*UC Irvine, USA*

## Abstract

Understanding of the parton distributions at small  $x(g)$  is one of the most important issues for clarifying of the QCD basics. In this paper potential of the LHeC for probing small  $x(g)$  region via  $c\bar{c}$  and  $b\bar{b}$  production has been investigated. Comparison of the  $ep$  and real  $\gamma p$  options of the LHeC clearly show the advantage of  $\gamma p$  collider option. Measurement of  $x(g)$  down to  $3 \times 10^{-6}$  with high statistics, especially at  $\gamma p$  option, seems to be reachable which is two order smaller than HERA coverage.

## 1 Introduction

The problem of precise measurement of parton distribution functions (PDF) is yet to be solved for the energy scales relevant to the LHC results. On the other hand, precision knowledge on the parton distribution of small  $x_B$  and sufficiently large  $Q^2$  is crucial for enlightening the QCD basics at all levels, from partons to nuclei. Besides, with the recent discovery of the 125 GeV scalar particle [1], [2] at the LHC, the basic components of the electroweak part of the Standard Model (SM) have been completed. However, the Higgs mechanism provides less than 2% of mass of the visible universe. Remaining 98% are provided by the QCD part of the SM. Therefore, clarifying of the basics of the QCD is important for a better understanding of our universe. That's why the QCD explorer was proposed ten years ago (see review [3] and references therein). One of the required measurements is the gluon PDF for low momentum fraction: small  $x(g)$ . The last machine that has probed  $x(g)$  was HERA which had a reach of about  $x(g) > 10^{-4}$ . Large Hadron-Electron Collider (LHeC) project [4] - the most powerful microscope ever designed - will provide a unique opportunity to probe extremely small  $x(g)$  region. In this project, where proton-electron collisions are aimed the  $e - beam$  can be obtained from a new circular or linear machine.

Today, LR option is considered as the basic one for the LHeC [5]. Actually this decision was almost obvious from the beginning due to the complications in constructing by-pass tunnels around the existing experimental caverns and installing the  $e - ring$  in the already commissioned tunnel. Let us remind that the CDR stage of the LHC assumed also  $ep$  collisions using the already existed LEP ring; but it turned out that LHC installation required dismantling of LEP from the tunnel.

Within the linac-ring option of the LHeC, a proton beam from LHC can be hit with a high energy electron or photon beam. The photons may be virtual ones from the electron beam resulting in a typical DIS event or these can be real photons originating from the Compton Back Scattering process. In the latter case, the photon spectrum consists of the high energy photons peaking at about 80% of the electron beam energy on the continuum of Weizsacker-Williams photons. The present study aims to investigate the feasibility of a small  $x(g)$  measurement with such a machine. Main parameters of  $ep$  and  $\gamma p$  options of the LHeC are presented in section 2. Section 3 is devoted to investigation of small  $x(g)$  region using the processes  $\gamma p \rightarrow c\bar{c}X$  and  $\gamma p \rightarrow b\bar{b}X$ . The generator level results are obtained using CompHEP [6] software package. Comparison with processes  $ep \rightarrow ec\bar{c}X$  and  $ep \rightarrow eb\bar{b}X$  shows an obvious advantage of the LHeC  $\gamma p$  option, which will provide more than one order higher cross sections at small  $x(g)$  region comparing to the  $ep$  option. Finally, section 4, provides a summary of the conclusion together with some suggestions.

## 2 Main parameters of $ep$ and $\gamma p$ options of the LHeC

It should be emphasized that real  $\gamma p$  collisions can be achieved only on the base of linac ring type  $ep$  colliders (see review [7] for history and status of linac-ring type collider proposals). Real  $\gamma$  beam for  $\gamma p$  collider [8], [9], [10], [11] will be produced using the Compton back scattering of laser beam off the high energy electron beam [12], [13]. Possible application of this mechanism to the other LHeC option under consideration, namely to ring-ring type  $ep$  colliders results in negligible  $\gamma p$  luminosities,  $L_{\gamma p} < 10^{-7} L_{ep}$ .

Currently, two versions for the  $ep$  option of the LHeC are under consideration: multi-pass energy recovery linac (ERL) yielding  $L_{ep} = 10^{33} cm^{-2} s^{-1}$  and pulsed single pass linac yielding  $L_{ep} = 10^{32} cm^{-2} s^{-1}$ . In the first case,  $E_e = 60 GeV$  has been chosen as a base electron energy, since higher energies are not available because of the synchrotron radiation loss in the arcs. In the second case, beam energies above 140 GeV would be available [4]. These two options will be denoted as LHeC-1 and LHeC-2. Main parameters of the LHeC  $ep$  collisions, in different options are presented in Table 1.

Table 1: Main parameters of ep collisions.

	$E_e, GeV$	$E_p, TeV$	$\sqrt{s}, TeV$	$L, cm^{-2}s^{-1}$
ERL	60	7	1.30	$10^{33}$
LHeC-1	60	7	1.30	$9 \times 10^{31}$
LHeC-2	140	7	1.98	$4 \times 10^{31}$

In the  $\gamma p$  option the luminosity of  $\gamma p$  collisions will be similar to the luminosity of  $ep$  collisions for the pulsed single straight linac. In the ERL case,  $L_{\gamma p}$  will be 10 times lower than  $L_{ep}$  as the energy recovery does not work after Compton back scattering.

### 3 Inclusive processes yielding $c\bar{c}$ and $b\bar{b}$ final states at LHeC

The final states that can be easily distinguished from the background events and that would give a good measure of the  $x(g)$  are  $eg \rightarrow eq\bar{q}$  and/or  $\gamma g \rightarrow q\bar{q}$  where the gluon ( $g$ ) is from the LHC protons, electrons and photons are from a new accelerator (namely, an electron linac providing beams tangential to the LHC) to be build and the letter  $q$  stands for a heavy quark flavour, such as  $b$  quark and possibly  $c$  as well. The  $b$  quark final states are easier to identify due to  $b$ -tagging possibility using currently available technologies: for example, ATLAS silicon detectors have about 70%  $b$ -tagging efficiency. In Table 2 we present the cross sections for heavy quark pair production via DIS, quasi real photons (WWA) and Compton Back Scattering (CBS) photons at the LHeC with  $E_e = 60 GeV$  and  $E_e = 140 GeV$ . For comparison, we also give values for DIS and WWA processes at HERA. It is seen that WWA quasi real photons are advantageous comparing to DIS and CBS photons are advantageous comparing to WWA. All numerical calculations are performed using CompHep [6] with CTEQ6L1 [14] PDF distributions. In Figure 1, the differential cross section depending on the  $x(g)$  has been shown for WWA photons at HERA and at LHeC. As expected, LHeC will give opportunity to investigate an order smaller  $x(g)$  than HERA.

Table 2: Heavy quark pair production cross sections via DIS, WWA, and CBS mechanisms.

Machine	$b\bar{b} (pb)$			$c\bar{c} (pb)$		
	DIS	WWA	CBS	DIS	WWA	CBS
HERA	$6.07 \times 10^2$	$4.57 \times 10^3$	-	$4.66 \times 10^4$	$7.29 \times 10^5$	-
LHeC-1( $E_e = 60 GeV$ )	$4.26 \times 10^3$	$2.99 \times 10^4$	$2.41 \times 10^5$	$2.38 \times 10^5$	$3.44 \times 10^6$	$2.38 \times 10^7$
LHeC-2( $E_e = 140 GeV$ )	$7.07 \times 10^3$	$4.91 \times 10^4$	$3.70 \times 10^5$	$3.72 \times 10^5$	$5.27 \times 10^6$	$3.46 \times 10^7$

The advantage of the CBS photons becomes even more obvious if one analyzes  $x(g)$  distribution of differential cross sections for CBS, WWA and DIS. In Figure 2, we show the  $d\sigma/dx(g)$  at the LHeC-1 for  $c\bar{c}$  production. It is seen that CBS at small  $x(g)$  region provides more than one (two) order higher cross sections comparing to WWA (DIS). For example, differential cross section of  $c\bar{c}$  pair production at the LHeC-1 achieves maximum value  $94 \mu b$  at  $x(g) = 1.44 \times 10^{-5}$  for CBS, whereas maximum value for WWA and DIS are  $4 \mu b$  at  $x(g) = 1.54 \times 10^{-5}$  and  $0.15 \mu b$  at  $x(g) = 3.89 \times 10^{-5}$ , respectively. Similar distributions for  $b\bar{b}$  at LHeC-1,  $c\bar{c}$  at LHeC 2 and  $b\bar{b}$  at LHeC-2 are shown in Figures 3, 4 and 5, respectively. Maximum values of differential cross sections and corresponding  $x(g)$  values for DIS, WWA, and CBS at the LHeC-1 (2) are given in the Table 3 (4). The advantage of CBS due to large cross section is obvious from the comparison.

Table 3: Maximum values of differential cross sections and corresponding  $x(g)$  values for DIS, WWA, and CBS at the LHeC-1.

	$c\bar{c}$		$b\bar{b}$	
	$d\sigma/dx$	$x$	$d\sigma/dx$	$x$
DIS	$0.15 \mu b$	$3.89 \times 10^{-5}$	$0.47 nb$	$1.99 \times 10^{-4}$
WWA	$4.0 \mu b$	$1.54 \times 10^{-5}$	$5.02 nb$	$1.25 \times 10^{-4}$
CBS	$94 \mu b$	$1.44 \times 10^{-5}$	$117 nb$	$1.23 \times 10^{-4}$

Table 4: Maximum values of differential cross sections and corresponding  $x(g)$  values for DIS, WWA, and CBS at the LHeC-2.

	$c\bar{c}$		$b\bar{b}$	
	$d\sigma/dx$	$x$	$d\sigma/dx$	$x$
DIS	$0.44 \mu b$	$1.54 \times 10^{-5}$	$1.73 nb$	$9.12 \times 10^{-5}$
WWA	$13.2 \mu b$	$6.45 \times 10^{-6}$	$17 nb$	$5.88 \times 10^{-5}$
CBS	$312 \mu b$	$6.02 \times 10^{-6}$	$408 nb$	$5.01 \times 10^{-5}$

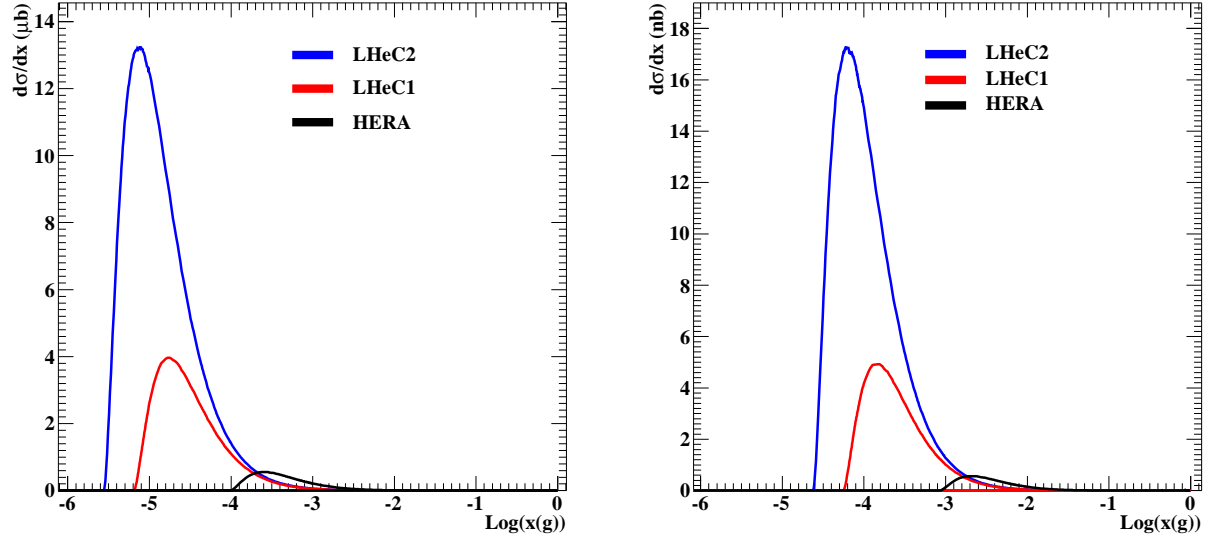


Figure 1: The  $x(g)$  reach and differential cross sections in  $c\bar{c}$  (left) and  $b\bar{b}$  (right) final states for the HERA and the LHeC.

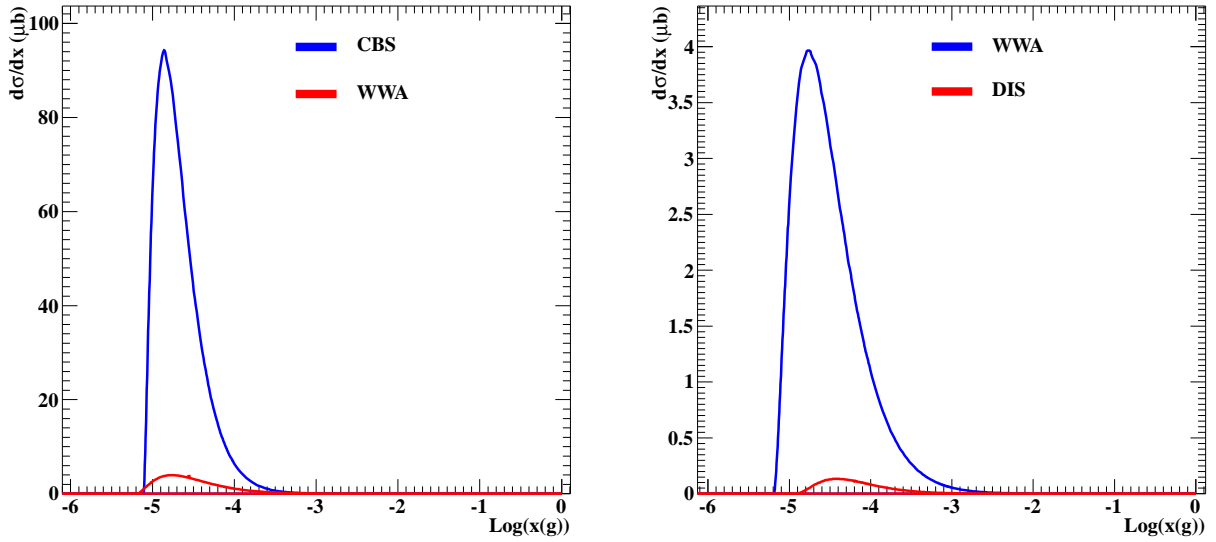


Figure 2: Differential cross sections for  $c\bar{c}$  final states produced via CBS, WWA and DIS at the LHeC-1.

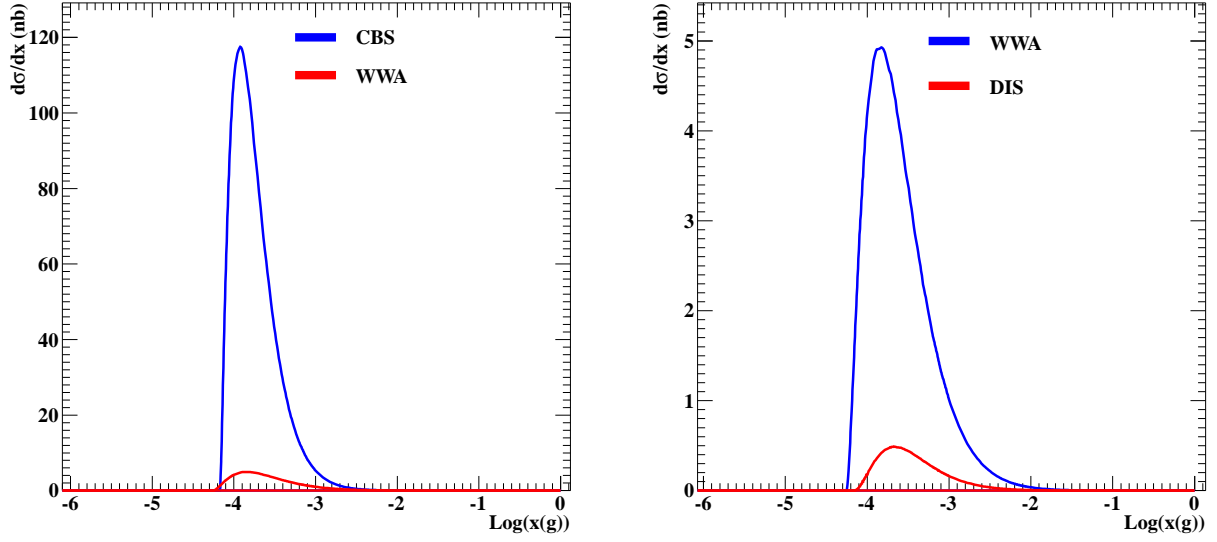


Figure 3: Differential cross sections for  $b\bar{b}$  final states produced via CBS, WWA and DIS at the LHeC-1.

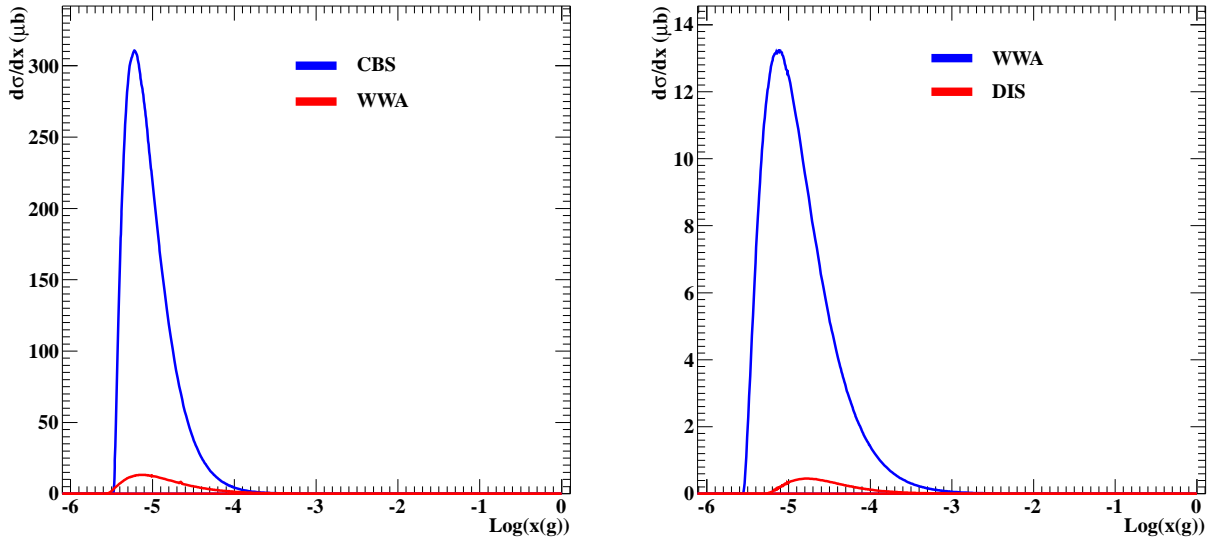


Figure 4: Differential cross sections for  $c\bar{c}$  final states produced via CBS, WWA and DIS at the LHeC-2.

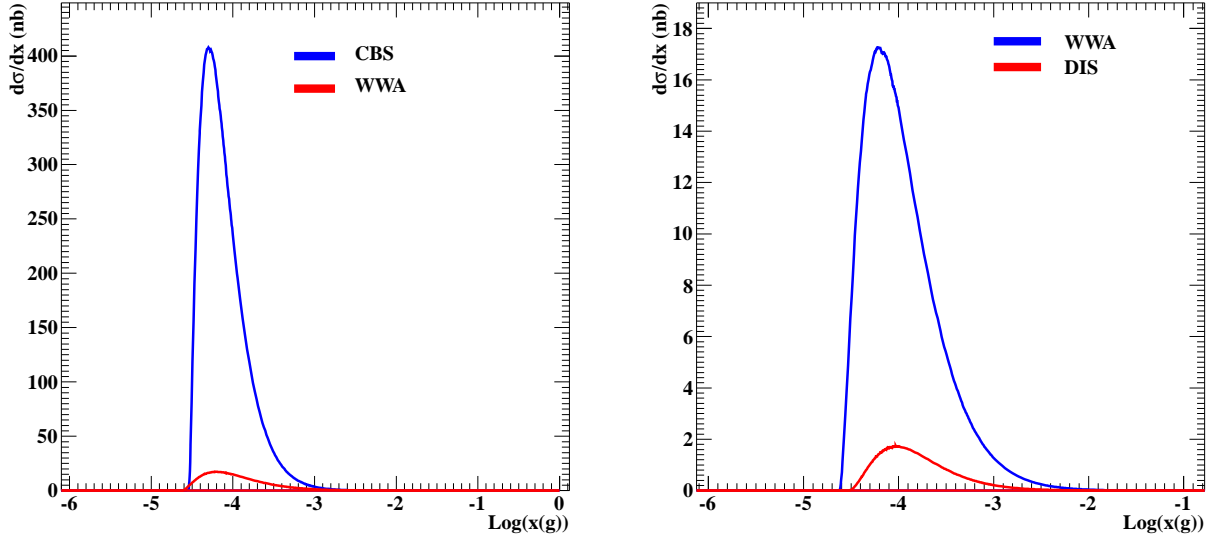


Figure 5: Differential cross sections for  $b\bar{b}$  final states produced via CBS, WWA and DIS at the LHeC-2 .

The angular dependency of the relevant processes is important to estimate the necessary  $\eta$  coverage of the detector to be built and also to estimate the eventual electron machine selection. For illustration we consider  $d\sigma/d\theta$  distribution where  $\theta$  is the angle between  $c$  ( $b$ ) quark and proton beam direction. These distributions for CBS at the LHeC-1 and LHeC-2 are presented in Figures 6 and 7, respectively. In Table 5, we present reachable  $x(g)$  for different  $\theta$  coverage. One can notice that even for an angular loss of about 5 degrees, there is considerable drop in both the cross section and in the  $x(g)$  reach. This effect can be understood by considering the  $\eta$  dependence of the heavy quark pair production cross section in  $\gamma p$  collisions which are shown in Figure 8 and 9. The vertical solid line is representative for a 1 degree, the dashed line for a 5 degree and the dot-dashed line is for 10 degree detector. Therefore, in order to have a good experimental reach the tracking should have an  $\eta$  coverage up to 5.

Table 5: Reachable  $x(g)$  for different  $\theta$  coverage.

	LHeC-1		LHeC-2	
$\theta$	$c\bar{c}$	$b\bar{b}$	$c\bar{c}$	$b\bar{b}$
0 – 180	$7.94 \times 10^{-6}$	$6.91 \times 10^{-5}$	$3.16 \times 10^{-6}$	$3.02 \times 10^{-5}$
1 – 179	$8.31 \times 10^{-6}$	$6.91 \times 10^{-5}$	$3.36 \times 10^{-6}$	$4.36 \times 10^{-5}$
5 – 175	$1.44 \times 10^{-5}$	$7.94 \times 10^{-5}$	$1.20 \times 10^{-5}$	$4.78 \times 10^{-5}$
10 – 170	$2.39 \times 10^{-5}$	$1.00 \times 10^{-4}$	$2.28 \times 10^{-5}$	$7.58 \times 10^{-5}$

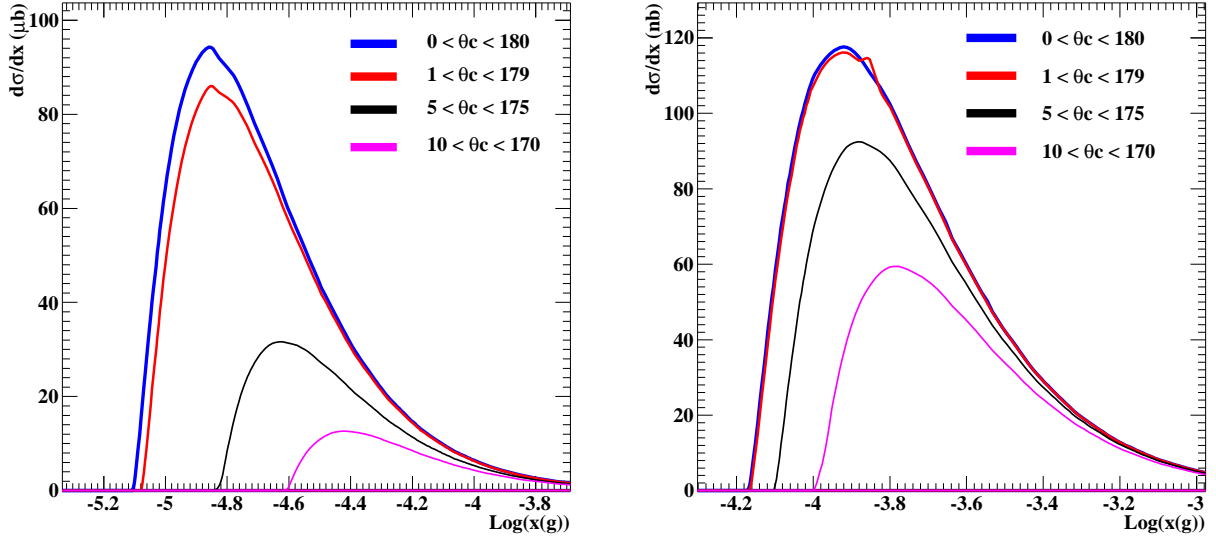


Figure 6: The effect of angular reach for  $c\bar{c}$  (left) and  $b\bar{b}$  (right) final states produced via CBS at the LHeC-1.

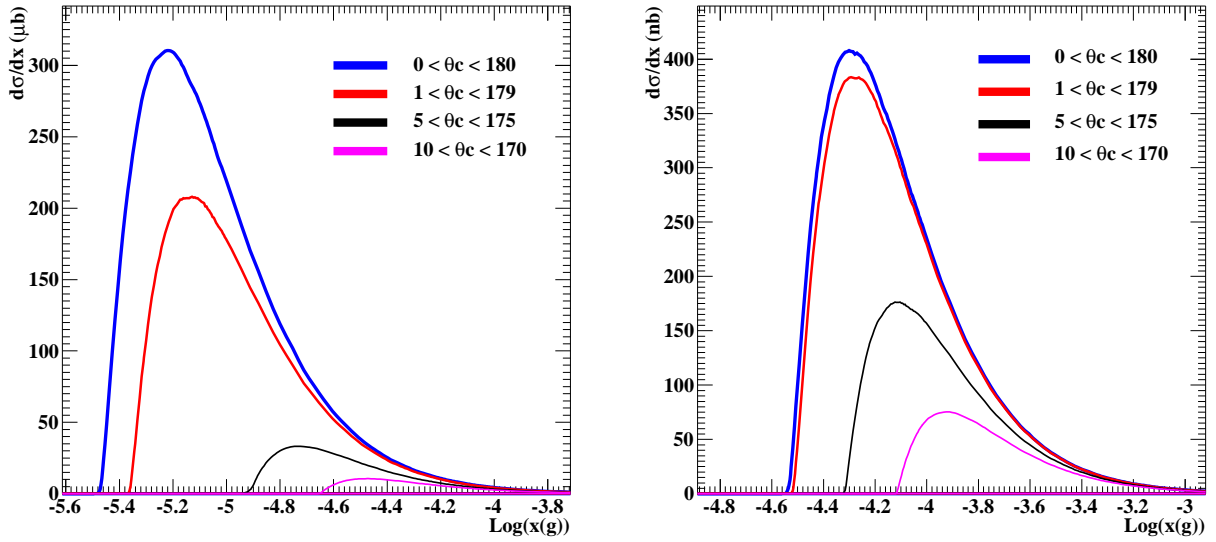


Figure 7: The effect of angular reach for  $c\bar{c}$  (left) and  $b\bar{b}$  (right) final states produced via CBS at the LHeC-2.

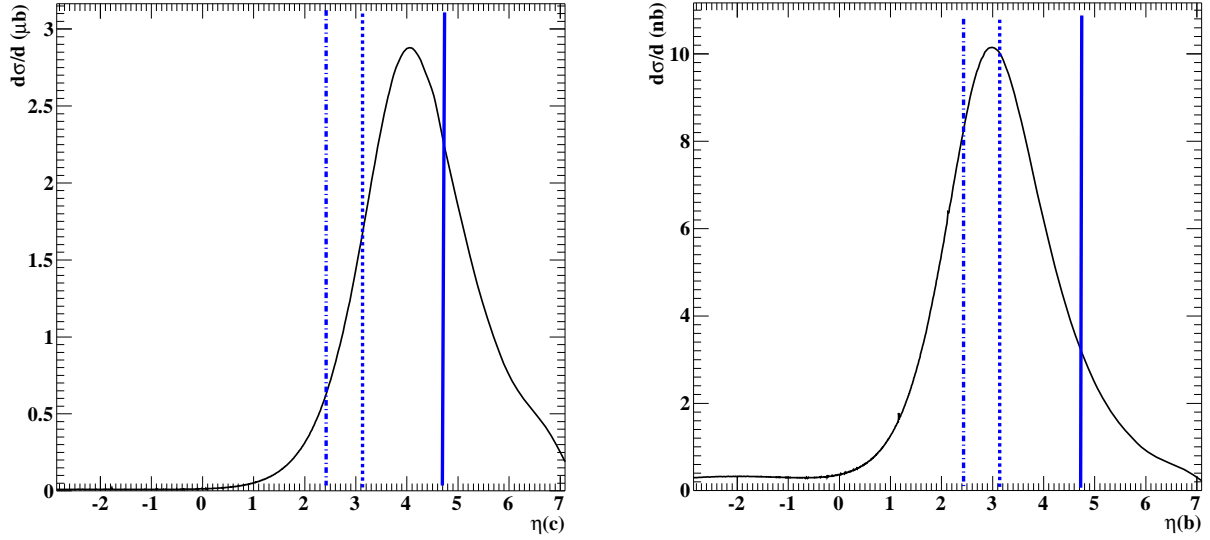


Figure 8: The  $\eta$  dependency of the  $c\bar{c}$  (left) and  $b\bar{b}$  (right) production cross section via CBS at the LHeC-1. Vertical lines represent  $1^\circ$  (solid line),  $5^\circ$  (dashed line) and  $10^\circ$  (dot-dashed line) detector cuts.

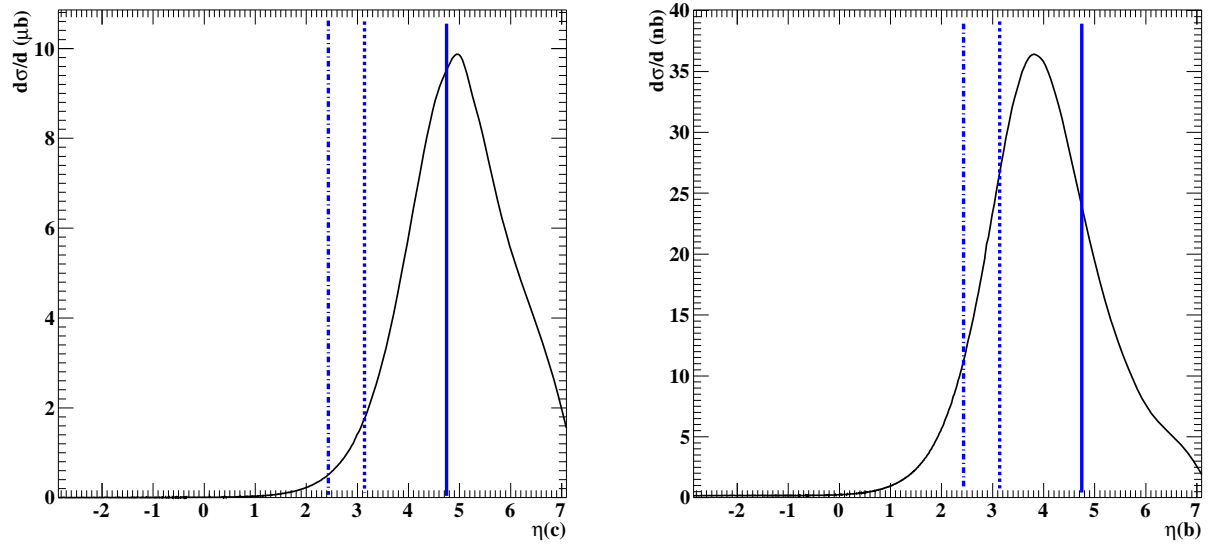


Figure 9: The  $\eta$  dependency of the  $c\bar{c}$  (left) and  $b\bar{b}$  (right) production cross section via CBS at the LHeC-2. Vertical lines are same as in Fig. 8.

## 4 Conclusions

Measurements of  $x(g)$  down to  $3 \times 10^{-6}$  seem to be reachable in  $\gamma p$  collisions which is two order smaller than the HERA coverage. These collisions provide higher cross section and better  $x(g)$  reach with respect to the  $ep$  collisions with the same electron beam energy. For the low  $x(g)$  region, the enhancement factor compared to the DIS  $ep$  collisions is about 700 for  $c\bar{c}$  final states and about 230 for  $b\bar{b}$  final states at the LHeC-2. Therefore, for the final states with heavy quarks, even if the  $\gamma p$  luminosity is 10 times smaller than  $ep$  luminosity (ERL option), the expected number of events in  $\gamma p$  collisions would be 70 and 20 times higher than in  $ep$  collisions for  $c\bar{c}$  and  $b\bar{b}$  final state respectively. The enhancement factor compared to WWA  $ep$  collisions is about 24 for both final states. The angular sensitivity is very important for smallest  $x(g)$  reach for either  $e$  or  $\gamma$  beams, therefore a detector with a pseudorapidity coverage up to  $\eta = 5$  is required. This coverage is already achieved at the ATLAS and CMS experiments using forward detector components.

Finally,  $ep$  option of LHeC will give an opportunity to shed light on the small  $x(g)$  dynamics which is crucial for clarifying the QCD basics. On the other hand, the  $\gamma p$  option of LHeC will essentially enlarge the LHeC capacity on the subject. Therefore, one pulse linac should be considered as a baseline for LHeC design. In this case, a higher center of mass energies can be achieved

by lengthening of the electron linac which will provide an opportunity to investigate smaller  $x(g)$  region. The luminosity loss can be compensated using energy recovery linac without re-circulating arcs [15] which may provide luminosity values exceeding  $L = 10^{34} \text{ cm}^{-2} \text{ s}^{-1}$  even with a multi-hundred GeV electron linac.

## References

- [1] ATLAS collaboration, G. Aad et al., *Combined search for the standard model Higgs boson using up to  $4.9 \text{ fb}^{-1}$  of  $pp$  collision data at  $\sqrt{s} = 7 \text{ TeV}$  with ATLAS detector at the LHC*, *Phys. Lett. B* **710** (2012) 49 [arxiv:1202.1408].
- [2] CMS collaboration, S. Chatrchyan et al., *Combined results of searches for the standard model Higgs boson in  $pp$  collisions at  $\sqrt{s} = 7 \text{ TeV}$* , *Phys. Lett. B* **710** (2012) 26 [arxiv:1202.1488].
- [3] S. Sultansoy, *Linac-ring type colliders: Second way to TeV scale*, *Eur Phys. J C* **33**, s01, s1064-s1066 (2004).
- [4] J.L.Abeleira Fernandez , C.Adolphsen , A.N.Akay et al., *A Large Hadron Electron Collider at CERN: Report on the Physics and Design Concepts for Machine and Detector*, *J. Phys. G: Nucl. Part. Phys.* **39** (2012) 075001.
- [5] J.L.Abeleira Fernandez , C.Adolphsen , P.Adzic et al., *A Large Hadron Electron Collider at CERN*, arXiv:1211.4831v1 [hep-ex] 20 Nov 2012.
- [6] E. Boos et al. (CompHEP Collaboration), *Automatic computations from Lagrangians to events*, *Nucl. Instrum. Meth. A* **534**, 250 (2004).
- [7] A. N. Akay, H. Karadeniz, and S.Sultansoy, *Review of Linac-Ring Type Collider Proposals*, *Int. J. Mod. Phys. A* **25**, 4589 (2010).
- [8] S. I. Alekhin et al., *PHYSICS AT gamma p COLLIDERS OF TeV ENERGIES*, *Int. J. Mod. Phys. A* **6**, 21 (1991).
- [9] A. K. Ciftci et al., *Main parameters of TeV energy  $\gamma - p$  colliders*, *Nucl. Instrum. Methods Phys. Res., Sect. A* **365**, 317 (1995).
- [10] A. K. Ciftci, S. Sultansoy, and O. Yavas, *TESLA \* HERA based  $\gamma - p$  and  $\gamma - A$  colliders*, *Nucl. Instrum. Methods Phys. Res., Sect. A* **472**, 72 (2001).
- [11] H. Aksakal et al., *Conversion efficiency and luminosity for  $\gamma - p$  colliders based on the LHC-CLIC or LHC-ILC QCD explorer scheme*, *Nucl. Instrum. Methods Phys. Res., Sect. A* **576**, 287 (2007).
- [12] I. F. Ginzburg et al., *Colliding gamma e and gamma gamma Beams Based on the Single Pass  $e^+ e^-$  Accelerators. 2. Polarization Effects. Monochromatization Improvement*, *Nucl. Instrum. Methods Phys. Res., Sect. A* **219**, 5 (1984).
- [13] V. I. Telnov, *Principles of photon colliders*, *Nucl. Instrum. Methods Phys. Res., Sect. A* **355**, 3 (1995).
- [14] J. Pumplin et al., *New generation of parton distributions with uncertainties from global QCD analysis*, *JHEP* **0207** (2002) 012.
- [15] V. Litvinenko, *LHeC with  $\sim 100\%$  energy recovery linac*, 2nd CERN-ECFA-NuPECC workshop on LHeC, Divonne-les-Bains 1-3 Sep (2009).